Petroleum Science 19 (2022) 688–696

Contents lists available at ScienceDirect

Petroleum Science

journal homepage: www.keaipublishing.com/en/journals/petroleum-science

Original Paper

Probing the effect of Young's modulus on the plugging performance of micro-nano-scale dispersed particle gels

Zhi-Xuan Zhu [a, b], Lin Li [a, b, **], Jia-Wei Liu [a, b], Jia Chen [a, b], Zhong-Zheng Xu [a, b], Yi-Ning Wu [a, b], Cai-Li Dai [a, b, c, *]

[a] Key Laboratory of Unconventional Oil & Gas Development (China University of Petroleum (East China)), Ministry of Education, Qingdao 266580, Shandong, China
[b] Shandong Key Laboratory of Oilfield Chemistry, Department of Petroleum Engineering, China University of Petroleum (East China), Qingdao 266580, Shandong, China
[c] State Key Laboratory of Heavy Oil Processing, China University of Petroleum (East China), Qingdao 266580, Shandong, China

ARTICLE INFO

Article history:
Received 26 May 2021
Accepted 14 October 2021
Available online 30 October 2021

Edited by Yan-Hua Sun

Keywords:
Dispersed particle gel
Mechanical strength
Young's modulus
Atomic force microscope
Plugging performance

ABSTRACT

The effect of mechanical strength of the dispersed particle gel (DPG) on its macro plugging performance is significant, however, little study has been reported. In this paper, DPG particles with different mechanical strengths were obtained by mechanical shearing of bulk gels prepared with different formula. Young's moduli of DPG particles on the micro and nano scales were measured by atomic force microscope for the first time. The mapping relationship among the formula of bulk gel, the Young's moduli of the DPG particles and the final plugging performance were established. The results showed that when the Young's moduli of the DPG particles increased from 82 to 328 Pa, the plugging rate increased significantly from 91.46% to 97.10% due to the distinctly enhanced stacking density and strength at this range. While when the Young's moduli of the DPG particles surpassed 328 Pa, the further increase of plugging rate with the Young's moduli of the DPG particles became insignificant. These results indicated that the improvement of plugging rate was more efficient by adjusting the Young's moduli of the DPG particles within certain ranges, providing guidance for improving the macroscopic application properties of DPG systems in reservoir heterogeneity regulation.

1. Introduction

Profile control and water shutoff have been employed as important techniques in highly efficient oilfield development. During the water flooding development process of oilfields, various chemical agents were applied to plug the high permeability zones to enhance flow resistance, diverting the injection fluid to flow into the low permeability zones, thereby enhancing the sweep efficiency and oil recovery efficiency. Polymer gel is a three-dimensional network structure constructed by chemical cross-linking of polymers in aqueous solution, which has been commonly used as a plugging agent because of its low cost and good adaptability (Al-Shajalee et al., 2020; Bai et al., 2015; Hajipour et al., 2018; Syed et al., 2014). Although the gel system has been well recognized as one of the most effective methods for profile control and water shutoff (Seright et al., 2021), it still suffers from uncontrollable gel strength in reservoir conditions and there lies a conflict between the migration distance and plugging strength (Ye et al., 2010; Jia et al., 2017). Therefore, the bulk polymer gels are prepared into dispersed particle gels (DPG) by physical shearing. The particles are dispersed in aqueous solution stably with low viscosity and controllable particle sizes, which are insusceptible to the shear of the pumping or the dilution of formation water during migration compared with the bulk gel (Dai et al., 2012; Zhao et al., 2013, 2017). In addition, the DPG particles deform elastically in the pore throat so that they can migrate to the deep part of the

* Corresponding author. Key Laboratory of Unconventional Oil & Gas Development (China University of Petroleum (East China)), Ministry of Education, Qingdao 266580, Shandong, China.
** Corresponding author. Key Laboratory of Unconventional Oil & Gas Development (China University of Petroleum (East China)), Ministry of Education, Qingdao 266580, Shandong, China.
E-mail addresses: lilin@upc.edu.cn (L. Li), daicl@upc.edu.cn (C.-L. Dai).

https://doi.org/10.1016/j.petsci.2021.10.027

reservoir. As compared with other water plugging and profile control agents, the DPG particles possess stronger deep fluid diversion ability and have been widely applied in controlling water cut in the late stage of reservoir development, making great contribution to stabilizing oil production (Zhao et al., 2015, 2018).

Plugging performance is taken as an important index to evaluate the application ability of the DPG particles in the oilfields, which is mainly affected by their intrinsic characteristics (Zhao et al., 2014). The impacts of physical properties such as the particle sizes and concentrations of the DPG particles on the plugging performance have been studied. Former studies have shown that the DPG particles plug the reservoir directly when the particle sizes are larger than the pore throat radii, while they deform through the pore throat and enter the deep part of the formation to plug the reservoir when the particle sizes are smaller than the pore throat radii (Dai et al., 2017). Moreover, great plugging effect can only be achieved at an appropriate concentration of DPG particles, as too high concentration will lead to excessive plugging in the near-well zone and the plugging effect of high permeability zones will be unsatisfactory when the concentration is too low (Zhao et al., 2018a,b). Although tremendous efforts have been dedicated to understanding the functions of DPG particles, the effect of mechanical properties of the DPG particles has not been studied systematically so far. DPG particles with different mechanical properties possess different resistance to deformation after being squeezed during the migration process, which would affect their plugging effects. The method based on GSC strength codes and method based on rheological parameters are generally used to characterize the strength of the bulk gels (Robert and Perry, 1988; Payro and Llacuna, 2006), however, little study has been conducted on characterizing the mechanical properties of the DPG particles. Micro-nano-scale Young's modulus can reflect the ability of the DPG particles to resist compression deformation when they migrate in the porous medium, which can quantify the mechanical properties of the DPG particles more accurately. Traditional methods for measuring Young's modulus include optical lever stretching method, pulse excitation method, and acoustic resonance method, etc. (Oral et al., 2011; Rubino and Loppolo, 2016; Saeki et al., 2011). However, the above-mentioned methods fail to characterize the mechanical properties of materials on micro-nano scale. With the development of nanomechanical measurement technology, atomic force microscope has emerged as an advanced method for measuring the Young's moduli of small-scale materials. Docheva et al. have used AFM to gain the mechanical properties of cells (Docheva et al., 2008). Young's modulus of polycrystalline titania microspheres has been determined by in-situ nanoindentation of AFM (Hao et al., 2014). Space-resolved quantitative mechanical measurements of soft and supersoft materials have been conducted by Galluzzi et al. (2016). Young's moduli of PS/mSiO_2 microspheres were also measured using the nano–indentation analysis of AFM to optimize the performance of hybrid materials (Chen et al., 2019).

In this paper, DPG particles with different mechanical properties were obtained by mechanical shearing of phenolic resin bulk gels prepared with different concentrations of polymers and cross-linkers. Young's moduli of DPG particles were measured by the atomic force microscope for the first time. The plugging performance of the DPG particles was obtained through core flow tests. The mapping relationship among the formula of bulk gel, Young's moduli of the DPG particles and the final plugging performance was established. The optimum range to adjust the Young's modulus of DPG to boost the plugging performance was proposed so that corresponding formula could be sought, providing guidance for further optimizing the effect of the DPG particles on reservoir heterogeneity control.

2. Experimental

2.1. Materials

P82-2 polyacrylamide (dry powder) with an average molecular weight of 14,000,000 and P87-5 phenolic resin cross-linker were both purchased from Shanghai Macklin Biochemical Co., LTD. The simulated formation water applied throughout the experiment was with a salinity of 10,000 mg/L (NaCl: 8500 mg/L; $CaCl_2$: 1000 mg/L; $MgCl_2$: 500 mg/L).

2.2. Preparation of bulk gels

Polymer solutions with six different concentrations of 0.2%, 0.25%, 0.3%, 0.35%, 0.4% and 0.45% were prepared using simulated formation water. Then 1.2, 1.4, 1.6. 1.8, 2.0 and 2.2 g of phenolic resin cross-linker were added respectively to 1000 mL of the above-mentioned polymer solutions and stirred to form 36 uniform gel solutions at room temperature. Then the uniform gel solutions were injected into ampoule bottles and sealed jars. After reaction at 90 °C for 24 h in an oven, bulk gel systems with different cross-linking densities and mechanical strengths were obtained.

2.3. Preparation of DPG particles

Bulk gel systems prepared above were mixed with simulated formation water at a ratio of 1:1, and poured into a colloidal mill (CM-2000 type, Shanghai Yiken Instruments Ltd., China). By controlling the rotation speed at a frequency of 20–60 Hz with 3–10 min of cyclic shearing, 36 systems of micro-nano-scale DPG particles with similar particle sizes were produced. The above experiments were all conducted at room temperature.

2.4. Characterization of strength of bulk gels

Gel Strength Codes (GSC) method was used to characterize the gel strength grade of the bulk gels systems in the ampoule bottles. Rheometer (Haake Mars60) was used to evaluate the storage moduli (G') of the bulk gel systems in the sealed jars. The rheology tests were conducted at 25 °C with an angular frequency (ω) of 6.28 rad/s. The linear viscoelastic region was determined first by stress scanning at 0.1 Hz in the oscillatory shear mode before the storage moduli of bulk gels were measured. The bulk gels were aged at 90 °C for 30 days, and the changes of the gel strength grades and storage moduli were measured every 5 days.

2.5. Characterization of Young's moduli of DPG particles

Atomic force microscope (AFM, Bruker Multimode 8) was used to analyze the Young's moduli of DPG particles. A spherical silica particle with a diameter of 5 μm was stick to the original tip of the probe SCANASYST-FLUID. The cantilever spring constant was calibrated as 0.06 N/m and the scan rate was set as 1 Hz. The micromorphology was scanned by Tapping mode of AFM. Then force-distance curves of center pixels of the spherical particles in the imaging process of DPG particles in liquid environment were recorded in real time. During the measurement, the distance between the probe and the DPG particles was equivalent to the deformation of the particle sample, which was signed as δ_s. PeakForce mode of AFM was used to measure the relationship curve between force and δ_s. The equivalent radius R of the probe and the sample was calculated using the following equation (Sun et al., 2004).

$$R = \frac{R_{tip} \cdot R_s}{R_{tip} + R_s}$$

where R_{tip} and R_s are the radius of the probe and the sample, respectively.

By fitting the force curves with the Johnson-Kendall-Roberts (JKR's) model, the Young's modulus E of the micro-nano-scale DPG particle system was calculated using the following equation (Tan et al., 2004; Cappello et al., 2020).

$$E = -\frac{3(1-\nu^2)}{4}\left(\frac{1+\sqrt[3]{16}}{3}\right)^{\frac{3}{2}} \cdot \frac{F_1}{\sqrt{R\delta_s{}^3}}$$

where ν is the Poisson ratio of the sample, $\nu = 0.3$; F_1 is the maximum adhesion force between the probe and the sample.

2.6. Plugging performance of DPG particle systems

Fig. 1 shows a schematic diagram of the experimental setup for water flooding. The initial permeability k_{w0} of the Φ25 mm × 200 mm sand-packed pipe was measured by water flooding experiment in the single-pipe physical model. Sand-packed pipes with porosity of about 40% and similar initial permeability of about 0.5 μm^2 were selected as simulation cores for testing. Dispersions with gel particle concentration of 0.1% were injected into the simulation cores with similar initial permeability at a speed of 0.5 mL/min for plugging until the liquid injection volume reached 1 pore volume (PV).

During this process, the permeability of the simulation core was k_{w1}. Afterwards, the subsequent water flooding was performed at a constant speed until the pressure at the output end of the sand-packing pipe became stable. The permeability k_{w2} of the simulation core during subsequent water flooding process was obtained by the pressure change at the injection end of the simulation core. The above experiments were all conducted at room temperature. The plugging capability of DPG particles to the large pore throats in the reservoir was characterized using the following equations:

$$k = \frac{Q\mu L}{A\Delta p}$$

$$R_p = \frac{k_{w0} - k_{w1}}{k_{w0}}$$

$$F_r = \frac{k_{w0}}{k_{w1}}$$

$$F_{rr} = \frac{k_{w0}}{k_{w2}}$$

where R_p is the plugging rate; F_r is the resistance coefficient, F_{rr} is the residual resistance factor.

3. Results and discussion

Gel forming performance of 36 gel systems (with 6 different polymer concentrations and 6 different cross-linker concentrations) was characterized. The representative experimental results of 6 groups were shown in Fig. 2. In Fig. 2a, when the concentration of polymer P82-2 was 0.2% and the concentration of cross-linker P87-5 was 0.6%, the gel strength was grade D based on the GSC standard, and the fluidity of this system was strong. Fig. 2b–e showed the changes in the gel strength grades of the bulk gels. As the concentrations of polymer and cross-linker increased, the crosslinking density of the bulk gel enhanced, with the macroscopic strength code gradually rising from D to G level. In Fig. 2f, when the concentration of the polymer reached 0.45% and the concentration of the cross-linker attained 1.1%, the gel strength was grade H. When the ampoule bottle was inverted, the gel hardly flowed and the surface was just slightly deformed.

The storage moduli G' of the bulk gels prepared above were further measured using a rheometer. As shown in Table 1 and Fig. 3,

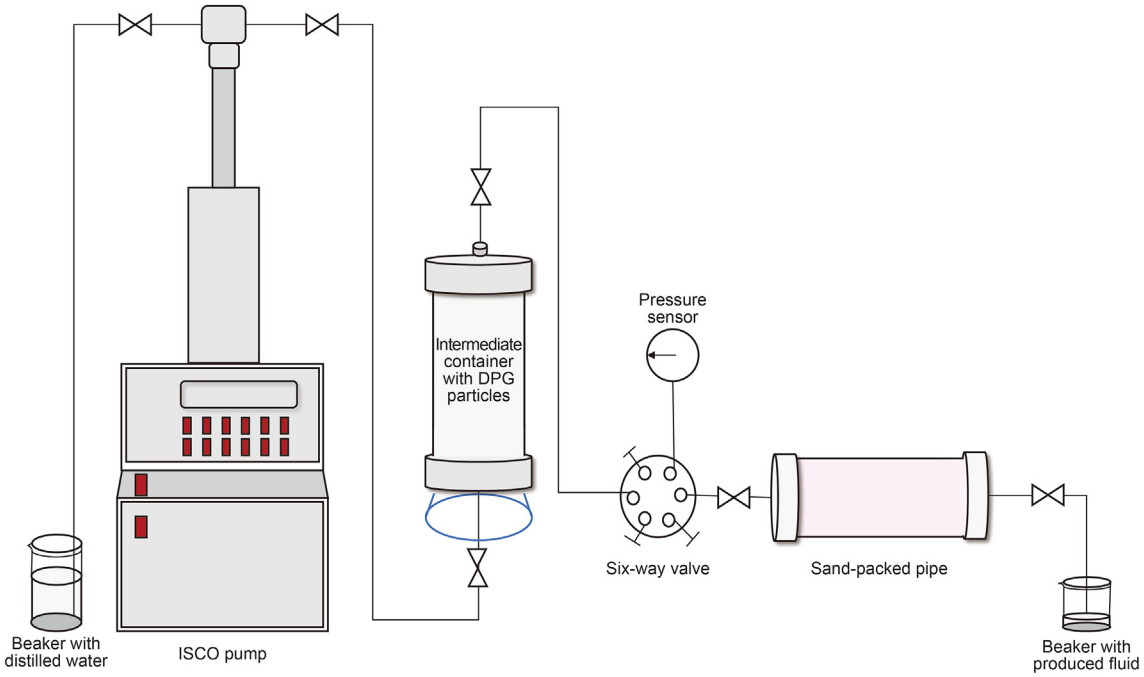

Fig. 1. The illustration of water flooding experiment setup.

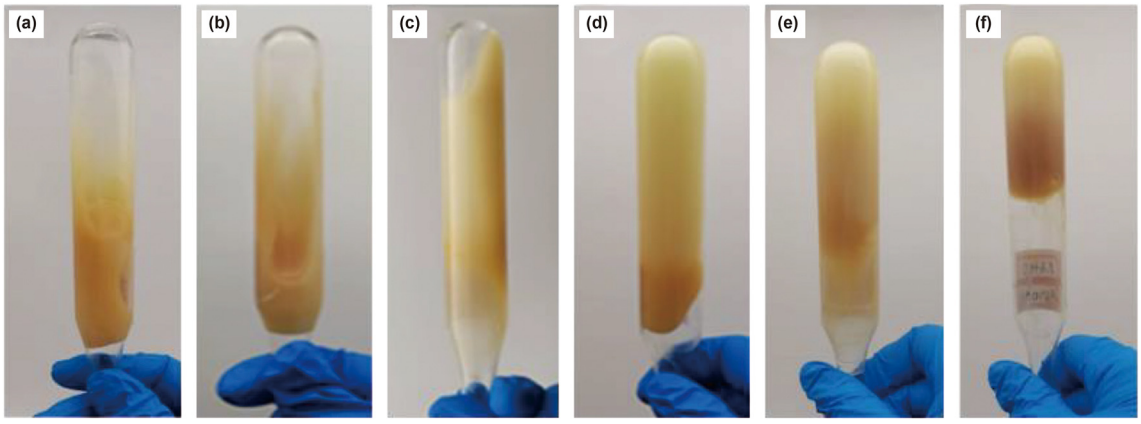

Fig. 2. Macro image showing strength of bulk gels. (**a**) 0.2% polymer + 0.6% cross-linker, (**b**) 0.25% polymer + 0.7% cross-linker, (**c**) 0.3% polymer + 0.8% cross-linker, (**d**) 0.35% polymer + 0.9% cross-linker, (**e**) 0.4% polymer + 1.0% cross-linker, (**f**) 0.45% polymer + 1.1% cross-linker.

Table 1
Storage moduli of bulk gels.

Cross-linker concentration, %	Storage modulus of bulk gels at different polymer concentrations, Pa					
	0.2%	0.25%	0.3%	0.35%	0.4%	0.45%
0.6	**0.96**	1.6	1.68	2.11	2.46	3.42
0.7	1.58	**1.71**	1.83	2.33	2.55	4.63
0.8	1.73	2.06	**2.17**	2.49	2.63	4.93
0.9	1.96	2.13	2.31	**3.17**	5.65	6.67
1.0	2.11	3.19	4.76	5.13	**5.82**	7.19
1.1	2.37	4.45	5.25	7.01	8.1	**9.73**

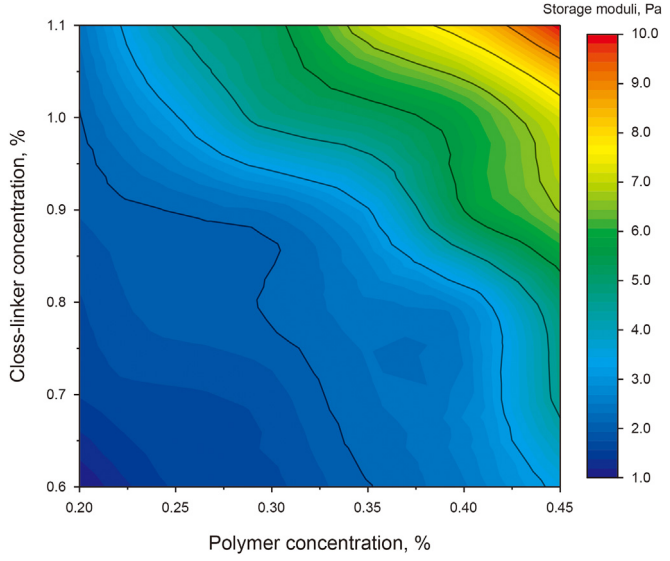

Fig. 3. The influence of concentrations of cross-linker and polymer on the storage moduli of bulk gels.

the storage moduli of the bulk gel systems were distributed from 1 to 10 Pa, all falling in the medium-strength gel regime. This result was consistent with that obtained from the previous GSC method.

When the polymer concentration was no higher than 0.4% and the cross-linker concentration was below 0.8%, with the increases in polymer and cross-linker concentrations, the storage moduli rose slowly from 0.96 to 2.63 Pa. This small increase rate could be attributed to the limited number of functional groups provided by the linear polymer and cross-linker involved in the reaction. Further increasing the concentrations of polymer and cross-linker, the storage moduli of the bulk gel enhanced significantly. This phenomenon could be explained from two aspects. On one hand, a large number of hydrophobic microdomains in the bulk gel systems facilitated the formation of abundant intermolecular-based associations; while on the other hand, the cross-linking points provided by the hydroxyl groups of phenolic resin were increased, both leading to denser physical network structure (Grattoni et al., 2001). Denser special structures facilitated more energies stored by deformation under the action of external force and more energies released after the elimination of external force, thereby enhancing the storage moduli of the phenolic resin bulk gels (Gu et al., 2018).

36 bulk gel systems presented no visible dehydration after aging for 90 days at 90 °C. Then storage moduli were used to evaluate the stability and experimental results of 6 representative systems were shown in Fig. 4. For bulk gels prepared with <0.35% polymer and <0.9% cross-linker, the gel strength maintained almost unchanged within the 90 days of aging. With further increasing the polymer and cross-linker concentrations, the changes of storage moduli of the bulk gels with aging time became more obvious. For bulk gel prepared with 0.45% polymer and 1.1% cross-linker, the storage

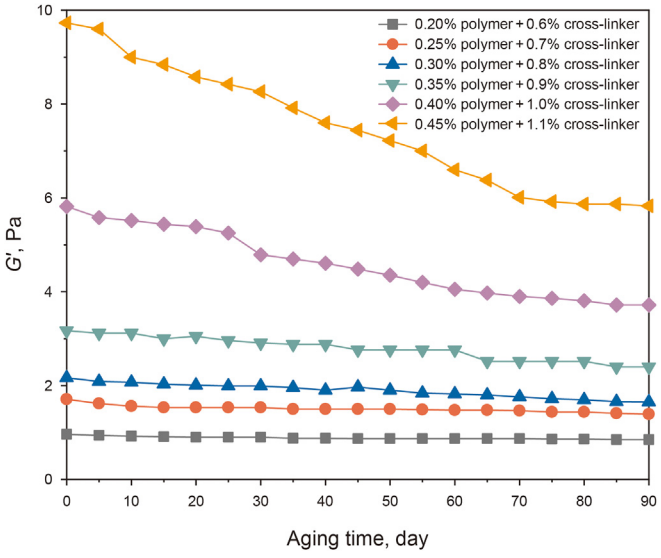

Fig. 4. The change trend of the strength of the bulk gel samples with aging time.

modulus decreased rapidly in the first 70 days (from 9.7 to 6.0 Pa), and changed slightly in the later days (eventually dropping to 5.83 Pa). These results could be explained that the dense structure in the bulk gel could slow the release rate of bound water to a certain degree (Nischang et al., 2013). However, when the cross-linking density was too large, the network and the volume of the bulk gel shrank, making it easier for water to separate out from the gel structure. Therefore, the storage moduli would drop more obviously (Brattekas, 2014; Liang et al., 2020).

Based on our experimental results, the prepared 36 bulk gel systems all exhibited good stability and could be used for long-term applications in reservoirs. Therefore 36 groups of DPG particles were prepared for the following studies. According to the results of the gel forming performance, it was found that for bulk gels with the same gel strength codes, their storage moduli were with apparent difference. For example, when the polymer concentration was controlled as 0.25% and the cross-linker concentration was increased from 0.7% to 1.1%, the strength codes of the prepared bulk gels were all characterized as level E by the GSC method; however, the storage moduli measured by the rheological method rose from 1.6 Pa to 4.45 Pa. Therefore, the difference in mechanical properties of the DPG particles prepared by shearing of the bulk gels with different storage moduli would further increase, which would affect the plugging effects of DPG particles in the reservoirs.

Tapping mode was applied first to obtain the microtopography of DPG particles. Experimental results of 6 representative groups were shown in Fig. 5. Small spheres with diameters around 1–2 μm could be clearly observed.

In order to measure the Young's moduli of the DPG particles, the force-distance curves were obtained by PeakForce mode of AFM. The probe tip was placed right in the center of a spherical particle and load was applied. Then the Young's modulus of the corresponding particle was obtained by fitting calculations (Johnson et al., 1971). Multiple groups of repeated tests were performed at each point and Fig. 6 demonstrated some representative force-distance curves.

It could be observed that the moduli were not single value but within certain range. Every time a force curve was taken, a modulus value could be obtained. The distribution percentages of Young's moduli in each statistical interval were obtained according to integration of data, thereby the histogram of interval distribution of Young's moduli of DPG particle system was drawn, as shown in Fig. 7a, with the peak of the Young's modulus distribution falling in the range of 80–100 Pa.

After multiplying the value of Young's modulus and its percentage in the distribution chart, the weighted average Young's modulus of every sample of DPG particles could be calculated, which was used to characterize the mechanical properties of the DPG particles. The results illustrated in Table 2 showed that the weighted average Young's modulus value of the micro-nano-scale DPG particles was at or near the peak of the distribution curves.

The Young's moduli of the micro-nano-scale DPG particles were obviously larger than the storage moduli of the macro-scale bulk gels, with even orders of magnitude difference. This difference was caused by the variation of the geometrical scale during the test, and the different physical principles on which the viscoelastic moduli data were based. On one hand, the variation of geometric scale will change the internal structure of the material thus affecting the mechanical properties (Rebelo et al., 2014; Wang and Liu, 2019; Bai et al., 2021). The sizes of the DPG particles are small. When the measured geometric scale is changed from the macro-scale to the micro-nano-scale, the electrostatic repulsion between the particles can be clearly sensed, which can strengthen the effect of surface stress and change the mechanical properties of the sample. At the same time, due to the large specific surface area of the micro-nano-scale DPG particles and the characteristics of high surface energy, the particles tend to aggregate to reduce the surface energy (You et al., 2014). As a result, the molecules and supramolecules in the aggregate state evolve towards ordering. On the other hand, their physical meanings are different. The storage modulus of the bulk gel was measured by dynamic shear rheometer under sinusoidal shear oscillation. It was used to represent the energy stored by

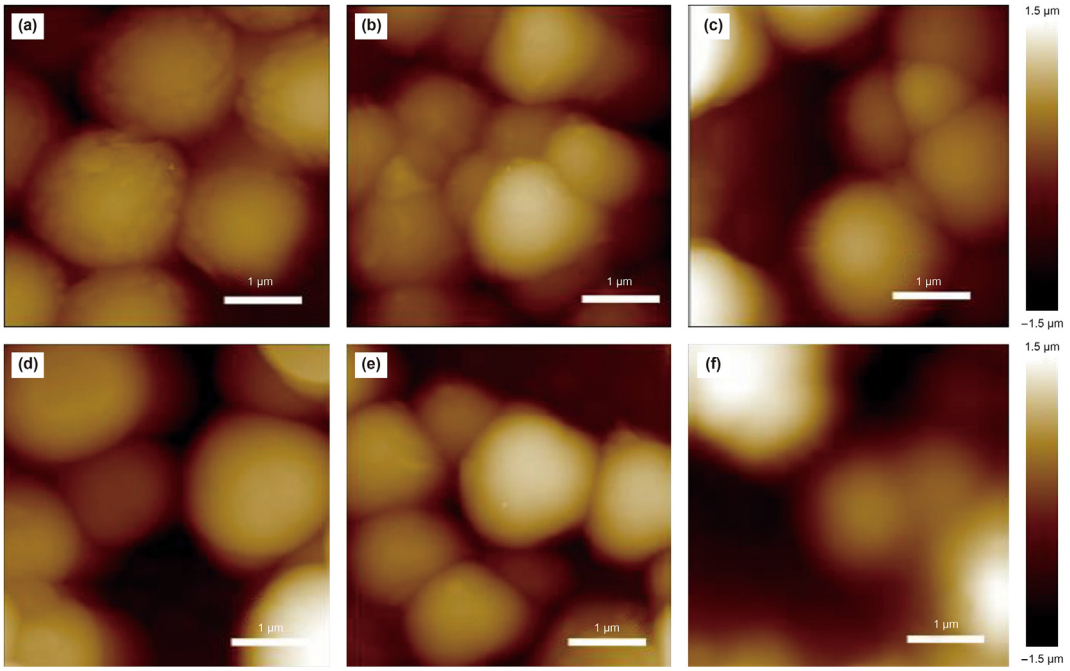

Fig. 5. Microscopic morphology of the micro-nano-scale DPG particle systems. (**a**) 0.2% polymer + 0.6% cross-linker, (**b**) 0.25% polymer + 0.7% cross-linker, (**c**) 0.3% polymer + 0.8% cross-linker, (**d**) 0.35% polymer + 0.9% cross-linker, (**e**) 0.4% polymer + 1.0% cross-linker, (**f**) 0.45% polymer + 1.1% cross-linker.

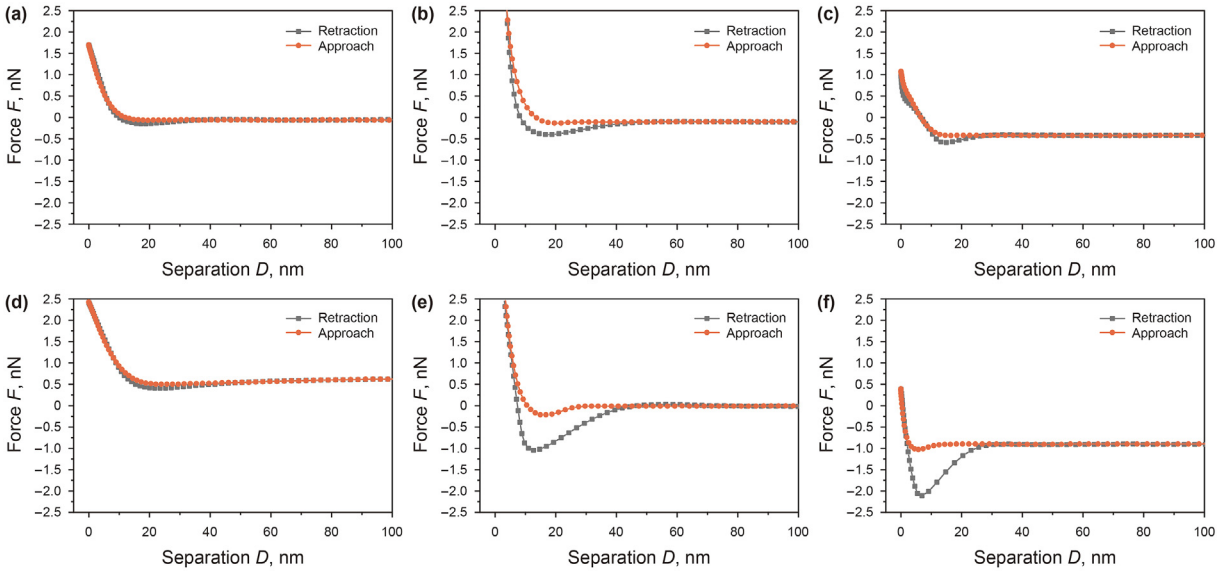

Fig. 6. Illustration of the force curves used to fit the Young's moduli of the DPG particles. (**a**) 0.2% polymer + 0.6% cross-linker, (**b**) 0.25% polymer + 0.7% cross-linker, (**c**) 0.3% polymer + 0.8% cross-linker, (**d**) 0.35% polymer + 0.9% cross-linker, (**e**) 0.4% polymer + 1.0% cross-linker, (**f**) 0.45% polymer + 1.1% cross-linker.

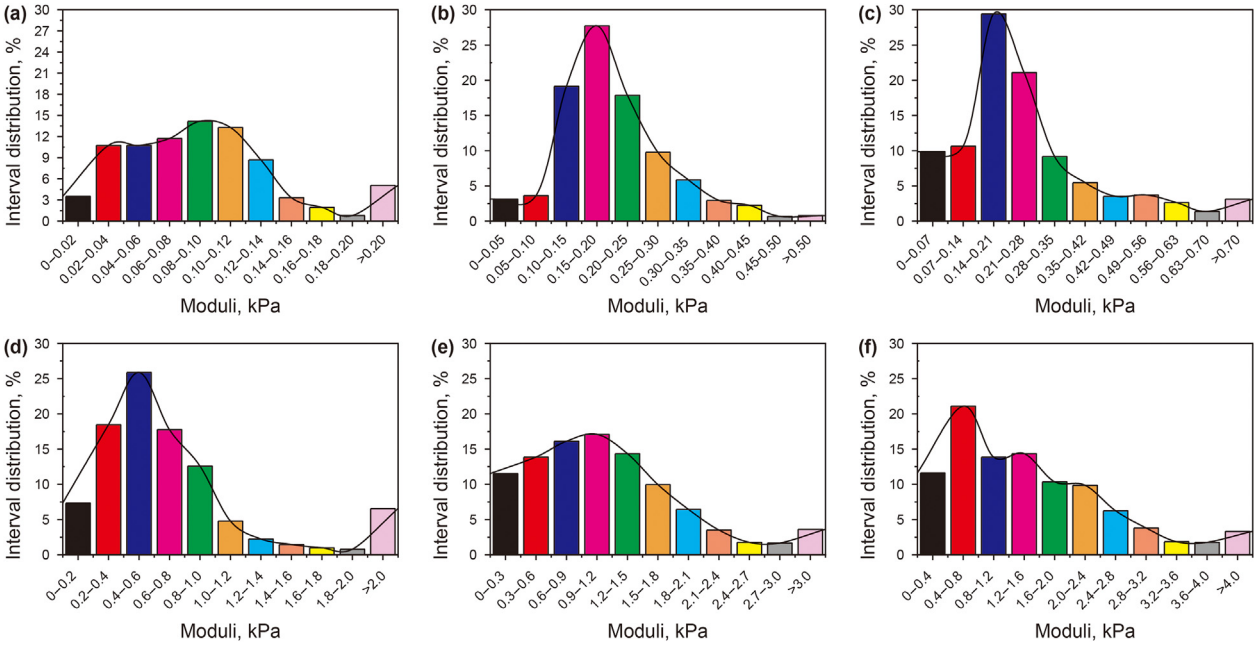

Fig. 7. Young's moduli distribution of the micro-nano-scale DPG particles systems. (**a**) 0.2% polymer + 0.6% cross-linker, (**b**) 0.25% polymer + 0.7% cross-linker, (**c**) 0.3% polymer + 0.8% cross-linker, (**d**) 0.35% polymer + 0.9% cross-linker, (**e**) 0.4% polymer + 1.0% cross-linker, (**f**) 0.45% polymer + 1.1% cross-linker.

Table 2
Young's moduli of DPG particle systems.

Cross-linker concentration, %	Young's modulus of DPG particles at different polymer concentrations, kPa					
	0.2%	0.25%	0.3%	0.35%	0.4%	0.45%
0.6	**0.082**	0.126	0.147	0.182	0.263	0.328
0.7	0.158	**0.19**	0.218	0.236	0.705	0.717
0.8	0.199	0.214	**0.257**	0.297	0.837	0.971
0.9	0.247	0.271	0.507	**0.762**	0.93	1.435
1.0	0.49	0.589	0.691	1.18	**1.222**	1.633
1.1	0.66	0.702	0.859	1.374	1.487	**1.723**

material during shear deformation process, which was equal to the elasticity of the bulk gel. While the Young's modulus of DPG particles was measured by atomic force microscope. External load was applied on the surface of the DPG particles directly during the measurement, and the Young's modulus represented the ability of the particles to withstand unidirectional compression deformation. During migrating in the porous medium, the soft dispersed particle gel would not be easily affected by the shear of the formation. However, it would be subjected to compression effects such as shape deformation during the plugging process and passing through the pore throat (Liu et al., 2016; Zhao et al., 2018a,b).

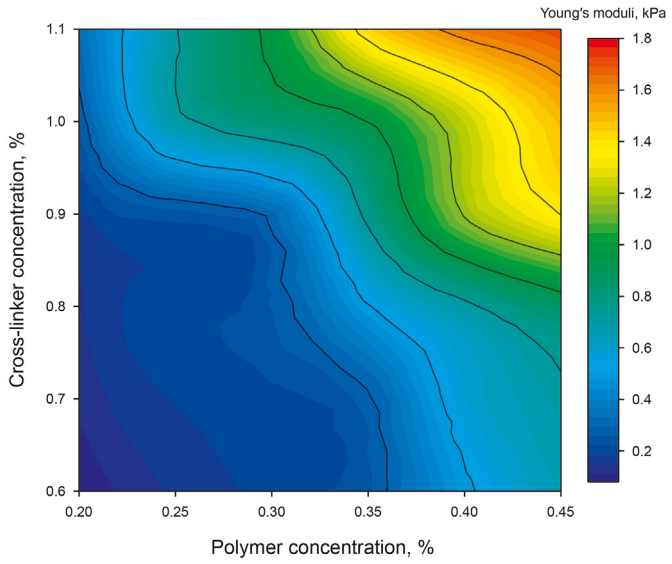

Fig. 8. The influence of concentrations of polymer and cross-linker on the Young's moduli of DPG particles systems.

Therefore, the Young's modulus of the DPG particles measured under compression can be used to characterize its mechanical strength more effectively and accurately.

Based on the results of Fig. 7 and Table 2, it was possible to draw a contour map of the changes of the Young's modulus of DPG particles with polymer and cross-linker concentrations. The concentrations of polymer and cross-linker corresponding to the DPG particles with same Young's moduli can be identified along one of the specific contour lines in Fig. 8. The distribution hierarchy and level of Young's moduli of DPG particles could be approximated by viewing the spacing of adjacent contour lines. In addition to the values represented by the contour lines, colors could also reflect the changes in the Young's moduli of the DPG particles more intuitively, As shown in Fig. 8, with warmer tones indicating higher moduli while cooler tones indicating smaller moduli.

Then the relationship between the Young's moduli of the DPG particles and the storage moduli of the bulk gels was established as shown in Fig. 9. It could be observed from Fig. 9 that the measured Young's moduli of the DPG particles and the storage moduli of the bulk gels could not be directly compared numerically under the combined influence of geometric scale and physical principles

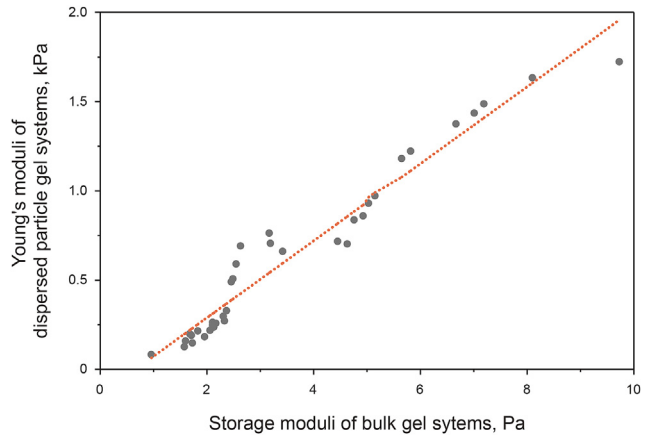

Fig. 9. Quantitative relationship between Young's moduli of the DPG particles and storage moduli of the bulk gels.

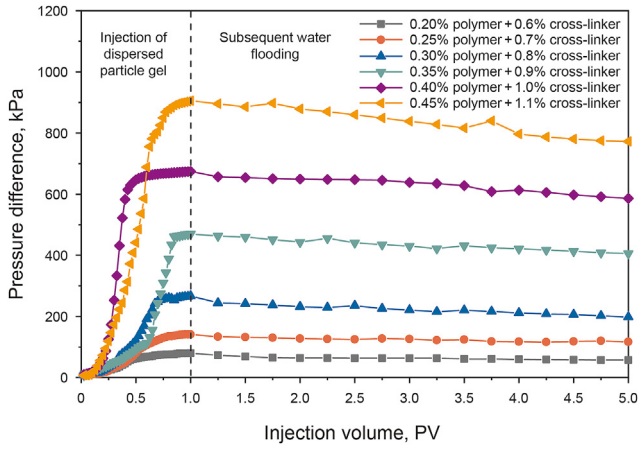

Fig. 10. Change of pressure difference with pore volume when injecting DPG particles.

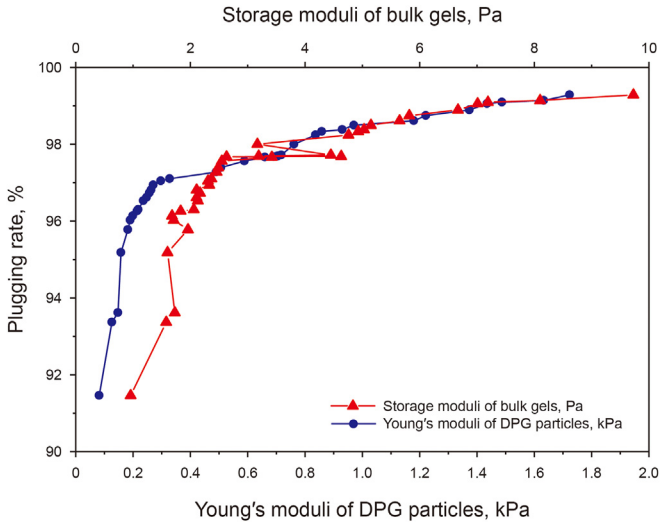

Fig. 11. Variation of plugging rate of DPG particles system.

mentioned above. However, the Young's moduli of the DPG particles basically increased linearly with the augment of the storage moduli of the bulk gels. Without considering the dimensions and the units, the storage modulus G' of bulk gel was taken as the independent variable and the Young's modulus E of the DPG particle was taken as the dependent variable to fit the following equation, where the goodness of fit R^2 was 0.9494.

$$E = 0.2162G' - 0.1429$$

This basically linear rising law could be explained that when the polymer or cross-linker concentrations increased, the intermolecular crosslinking density was greatly improved, resulting in denser spatial network structure of the bulk gels and enhanced mechanical strength. When preparing DPG particles from such kinds of bulk gels, the breaking fractures at the junctions of spherical particles were relatively reduced, thereby decreasing deformability of the particles. Accordingly, the Young's modulus of DPG particles measured under the same peak force would increase.

When micro-nano-scale DPG particles were plugged in the simulation core, changes of pressure differences of 6 representative systems were shown in Fig. 10. As the polymer and cross-linker concentrations increased, the Young's moduli of the DPG particles increased, and the peak value of the pressure difference rose from

Table 3
Plugging performance of DPG particles systems.

Formula of bulk gels	G' of bulk gels, Pa	E of DPG particle system, kPa	k_{w0}, μm^2	k_{w1}, μm^2	R_p, %	Peak value of F_r	Final value of F_{rr}
0.2% polymer +0.6% cross-linker	0.96	0.082	0.499	0.0426	91.46	11.71	8.47
0.25% polymer +0.7% cross-linker	1.71	0.190	0.483	0.0192	96.02	25.14	22.17
0.3% polymer +0.8% cross-linker	2.17	0.257	0.489	0.0160	96.73	30.60	25.24
0.35% polymer +0.9% cross-linker	3.17	0.762	0.522	0.0104	98.00	49.97	40.03
0.4% polymer +1.0% cross-linker	5.82	1.222	0.482	0.0060	98.75	79.88	69.55
0.45% polymer +1.1% cross-linker	9.73	1.723	0.523	0.0037	99.29	140.02	121.78

79.2 to 905.9 kPa. When the Young's moduli of the DPG particles were small (<257 Pa, with 0.3% polymer + 0.8% cross-linker in this case), the particles were easy to deform and pass through the pore throat to enter the deep part of the simulation cores. However, the accumulation of these soft particles in the pore throat was insignificant, and the increase in pressure was modest. When the Young's moduli of the DPG particles surpassed 762 Pa (with 0.35% polymer + 0.9% cross-linker in this case), the pressure increased rapidly with the injection of DPG particles, representing the increase in flow resistance in the pore throat structures. Particles with higher moduli preferentially entered the large pore throats and remained there. During the process of injection, the DPG particles gradually accumulated and bridged in the pore throats to plug. For all the 6 systems, the displacement pressure difference would continue to rise very slowly after reaching the breakthrough pressure, reducing the permeability of simulation cores effectively and ensuring the significance of subsequent water flooding. The displacement pressure differences after the subsequent water flooding with multiple pore volumes were still much larger than the initial pressures, indicating that all the DPG particle systems could form effective plugging and exhibited great flushing resistance performance.

The influences of Young's moduli of DPG particles on the plugging performance were shown in Fig. 11 and Table 3. For the 6 representative systems, the plugging rate to the stimulation cores all surpassed 90%, suggesting excellent plugging performance. Since suitable shear rate and shear time were chosen to prepare the DPG particles with similar sizes, the differences in plugging performance were mainly attributed to the effects of Young's moduli.

When the Young's moduli of the DPG particles increased from 82 to 328 Pa, the plugging rate increased significantly from 91.46% to 97.10%. At this moduli range, when the DPG particles passed through pore throats, they collided with each other elastically and deformed to form dense stacking. The stacking density and strength of DPG particles enhanced distinctly with the moduli, resulting in the significantly increased plugging rate. While when the Young's moduli of the DPG particles surpassed 328 Pa, the probability of relative movement among the particles was small due to the already dense packing. The shrinkage of the flow passage section in the pore throat reached critical state. Therefore, the plugging rate rose slowly with further increasing the Young's moduli of DPG particles.

The quantification results of the mechanical properties indicated that the plugging performance increased with the augment of Young's moduli of the DPG particles. This was consistent with the relationship of plugging rate varied with the storage modulus of the bulk gel, as illustrated in Fig. 11, proving the validity of the dimensionless formula ($E = 0.2162G' - 0.1429$). However, in consideration of the material cost, adjusting the Young's moduli of DPG particles within the range of 0.82–328 Pa would be more efficient in the practical application process. The establishment of the mechanical model of the Young's moduli of DPG system would provide guidance to the macro-scale application performance of the DPG particles.

4. Conclusions

In this study, Young's moduli of DPG particles on the micro and nano scales were measured by atomic force microscope for the first time. Young's moduli of the DPG systems basically showed a linear relationship with the augment of the storage moduli of the bulk gels. When the Young's moduli of the DPG particles increased from 82 to 328 Pa, the plugging rate increased significantly from 91.46% to 97.10%, as the stacking density and strength of DPG particles enhanced distinctly with the moduli at this range. While when the Young's moduli of the DPG particles surpassed 328 Pa, the enhancement of plugging rate with the Young's moduli became insignificant. The mapping relationship among the formula of bulk gel, the Young's moduli of the DPG particles and the final plugging performance was established. It was concluded that by adjusting the Young's moduli of the DPG systems within certain range, the increase in plugging rate would be more efficient. The studies in this paper provided guidance for improving the macroscopic application properties of DPG systems in reservoir heterogeneity regulation.

Acknowledgements

This work is financially supported by the National Key Research and Development Program of China (No. 2019YFA0708700), National Natural Science Foundation of China (52174054, 51804326), Shandong Provincial Natural Science Foundation (ZR2019BEE046).

References

Al-Shajalee, F., Arif, M., Machale, J., Verrall, M., Almobarak, M., Iglauer, S., Wood, C., 2020. A multiscale investigation of cross-linked polymer gel injection in sandstone gas reservoirs: implications for water shutoff treatment. Energy & Fuels 34 (11), 14046–14057. https://doi.org/10.1021/acs.energyfuels.0c02858.

Bai, B.J., Zhou, J., Yin, M.F., 2015. A comprehensive review of polyacrylamide polymer gels for conformance control. Petrol. Explor. Dev. 42, 525–532. https://doi.org/10.1016/S1876-3804(15)30045-8.

Bai, Y., Cao, G., Nan, X., 2021. Effect of sodium fluosilicate particles in acidification flowback fluid on emulsification stability of crude oil. J. Petrol. Sci. Eng. 202. https://doi.org/10.1016/j.petrol.2021.108484.

Brattekas, B., Hauge, A., Graue, A., Seright, R.S., 2014. Gel dehydration by spontaneous imbibition of brine from aged polymer gel. SPE J. 19 (1), 122–134. https://doi.org/10.2118/153118-MS.

Cappello, J., Herbemont, V., Lindner, A., Roure, O., 2020. Microfluidic in-situ measurement of Poisson's ratio of hydrogels. Micromachines 11 (3). https://doi.org/10.3390/mi11030318.

Chen, A., Chen, Y., Zhao, X.B., Wang, Y.Y., 2019. Core/shell structured PS/mSiO_2 hybrid particles: controlled preparation, mechanical property, and their size-dependent CMP performance. J. Alloys Compd. 779, 511–520. https://doi.org/10.1016/j.jallcom.2018.11.314.

Dai, C.L., Liu, Y.F., Zou, C.W., You, Q., Yang, S., Zhao, M.W., Wu, Y.N., Sun, Y.P., 2017. Investigation on matching relationship between dispersed particle gel (DPG) and reservoir pore-throats for in-depth profile control. Fuel 207, 109–120. https://doi.org/10.1016/j.fuel.2017.06.076.

Dai, C.L., Zhao, G., Zhao, M.W., You, Q., 2012. Preparation of dispersed particle gel (DPG) through a simple high speed shearing method. Molecules 17, 14484–14489. https://doi.org/10.3390/molecules171214484.

Docheva, D., Padula, D., Popov, C., Mutschler, W., Clausen, S.H., Schieke, M., 2008. Researching into the cellular shape, volume and elasticity of mesenchymal stem cells, osteoblasts and osteosarcoma cells by atomic force microscopy. J. Cell Mol. Med. 12, 537–552. https://doi.org/10.1111/j.1582-4934.2007.00138.x.

Galluzzi, M., Biswas, C.S., Wu, Y.H., Wang, Q., Du, B., Stadler, F.J., 2016. Space-

resolved quantitative mechanical measurements of soft and supersoft materials by atomic force microscopy. NPG Asia Mater. 8. https://doi.org/10.1038/am.2016.170.

Grattoni, C.A., Al-Sharji, H.H., Yang, C.H., Muggeridge, A.H., Zimmerman, R.W., 2001. Rheology and permeability of crosslinked polyacrylamide gel. J. Colloid Interface Sci. 240, 601–607. https://doi.org/10.1006/jcis.2001.7633.

Gu, C.L., Lyu, Y.H., Fan, X.Q., Zhao, C.X., Dai, C.L., Zhao, G., 2018. Study on rheology and microstructure of phenolic resin cross-linked nonionic polyacrylamide (NPAM) gel for profile control and water shutoff treatments. J. Petrol. Sci. Eng. 169, 546–552. https://doi.org/10.1016/j.petrol.2018.06.016.

Hajipour, A., Baghban Salehi, M., Vafaie Sefti, M., Heidari, A., 2018. Experimental study of polyacrylamide gel in close-in well operation. Polym. Adv. Technol. 29, 1278–1286. https://doi.org/10.1002/pat.4239.

Hao, P.D., Liu, Y.P., Du, Y.M., Zhang, Y.F., 2014. Young's modulus of polycrystalline titania microspheres determined by in situ nanoindentation and finite element modeling. J. Nanomater. 2014, 213. https://doi.org/10.1155/2014/309827.

Jia, H., Chen, H., Guo, S.S., 2017. Fluid loss control mechanism of using polymer gel pill based on multi-crosslinking during overbalanced well workover and completion. Fuel 210, 207–216. https://doi.org/10.1016/j.fuel.2017.08.032.

Johnson, K.L., Kendall, K., Roberts, A.D., 1971. Surface energy and the contact of elastic solids. Proc. Roy. Soc. Lond. 324, 301–313.

Liang, B., Wu, Q., Li, M., Yang, H.X., Yang, J., Jiang, H.Q., Li, J.J., 2020. Interplay between viscous pressure and capillary pressure on polymer gel dehydration and water shutoff in hydraulically fractured reservoirs. Energy & Fuels 34 (5), 5696–5706. https://doi.org/10.1021/acs.energyfuels.0c00368.

Liu, Y.F., Dai, C.L., Wang, K., Zhao, M.W., Zhao, G., Yang, Z., Fang, J.C., Wu, Y.N., 2016. Investigation on preparation and profile control mechanisms of the dispersed particle gels (DPG) formed from phenol formaldehyde cross-linked polymer gel. Ind. Eng. Chem. Res. 55, 6284–6292. https://doi.org/10.1021/acs.iecr.6b00055.

Nischang, I., 2013. Porous polymer monoliths: morphology, porous properties, polymer nanoscale gel structure and their impact on chromatographic performance. J. Chromatogr. A 1287, 39–58. https://doi.org/10.1016/j.chroma.2012.11.016.

Oral, I., Guzel, H., Ahmetli, G., 2011. Measuring the Young's modulus of polystyrene-based composites by tensile test and pulse-echo method. Polym. Bull. 67, 1893–1906. https://doi.org/10.1007/s00289-011-0530-z.

Payro, E.R., Llacuna, J.L., 2006. Rheological characterization of the gel point in sol–gel transition. J. Non-Cryst. Solids 352, 2220–2225. https://doi.org/10.1016/j.jnoncrysol.2006.03.001.

Rebelo, L.M., De Sousa, J.S., Abreu, A.S., Baronib, M.P.M.A., Alencarc, A.E.V., Soaresc, S.A.J., Mendes, F., Soaresd, J.B., 2014. Aging of asphaltic binders investigated with atomic force microscopy. Fuel 117, 15–25. https://doi.org/10.1016/j.fuel.2013.09.018.

Robert, D.S., Perry, A.A., 1988. Conformance improvement in a subterranean hydrocarbon-bearing formation using a crosslinked polymer. USP 93966686, 5–17. US4744419 A.

Rubino, E., Loppolo, T., 2016. Young's modulus and loss tangent measurement of polydimethylsiloxane using an optical lever. J. Polym. Sci. B Polym. Phys. 54, 747–751. https://doi.org/10.1002/polb.23972.

Saeki, I., Ohno, T., Sakai, O., Niya, T., Sato, T., 2011. In situ measurement of Young's modulus of FeO scale formed on pure iron at 973–1273 K by acoustic resonance method. Corrosion Sci. 53, 458–463. https://doi.org/10.1016/j.corsci.2010.09.057.

Seright, R., Brattekas, B., 2021. Water shutoff and conformance improvement: an introduction. Petrol. Sci. 18 (2), 450–478. https://doi.org/10.1007/s12182-021-00546-1.

Sun, Y.J., Akhremitchev, B., Walker, G.C., 2004. Using the adhesive interaction between atomic force microscopy tips and polymer surfaces to measure the elastic modulus of compliant samples. Langmuir 20, 5837–5845. https://doi.org/10.1021/la036461q.

Syed, A., Pantin, B., Durucan, S., Korre, A., Shi, J.Q., 2014. The use of polymer-gel solutions for remediation of potential CO_2 leakage from storage reservoirs. Energy Procedia 63, 4638–4645. https://doi.org/10.1016/j.egypro.2014.11.497.

Tan, S.S., Sherman, R.L., Ford, W.T., 2004. Nanoscale compression of polymer microspheres by atomic force microscopy. Langmuir 20 (17), 7015–7020. https://doi.org/10.1021/la049597c.

Wang, M., Liu, L.P., 2019. Aging behaviors of nanoscale mechanical properties of asphalt phases. J. Traffic Transport. Eng. 19, 1–13. https://doi.org/10.19818/j.cnki.1671-1637. 2019. 06.001 (in Chinese).

Ye, Z., He, B., , EQ, Xie, S.Y., Han, L.J., Chen, H., Luo, P.Y., Shu, Z., Shi, L.T., Lai, N.J., 2010. The mechanism study of disproportionate permeability reduction by hydrophobically associating water-soluble polymer gel. J. Petrol. Sci. Eng. 72, 64–66. https://doi.org/10.1016/j.petrol.2010.03.004.

You, Q., Tang, Y.C., Dai, C.L., Zhao, M.W., Zhao, F.L., 2014. A study on the morphology of a dispersed particle gel used as a profile control agent for improved oil recovery. J. Chem. 10. https://doi.org/10.1155/2014/150256, 6360–6360.

Zhao, G., Dai, C.L., Zhao, M.W., 2014. Investigation of the profile control mechanisms of dispersed particle gel. PLoS One 9 (9). https://doi.org/10.1371/journal.-pone.0100471, 100471–100471.

Zhao, G., Dai, C.L., Chen, A., Yan, Z.H., Zhao, M.W., 2015. Experimental study and application of gels formed by nonionic polyacrylamide and phenolic resin for in-depth profile control. J. Petrol. Sci. Eng. 135, 552–560. https://doi.org/10.1016/j.petrol.2015.10.020.

Zhao, G., Dai, C.L., Zhao, M.W., You, Q., Chen, A., 2013. Investigation of preparation and mechanisms of a dispersed particle gel formed from a polymer gel at room temperature. PLoS One 8, 1–9. https://doi.org/10.1371/journal.pone.0082651.

Zhao, G., Li, J.M., Gu, C.L., Sun, Y.P., Dai, C.L., 2018a. Dispersed particle gel strengthened polymer/surfactant as a novel combination flooding system for enhanced oil recovery. Energy & Fuels 32, 11317–11327. https://doi.org/10.1021/acs.energyfuels.8b02720.

Zhao, G., You, Q., Gu, C.L., Lv, Y.H., Dai, C.L., 2017. Preparation mechanism of multiscale dispersed particle gel. Acta Pet. Sin. 38, 821–829. https://doi.org/10.7623/syxb201707009 (in Chinese).

Zhao, G., You, Q., Tao, J.P., Gu, C.L., Aziz, H., Ma, L.P., Dai, C.L., 2018b. Preparation and application of a novel phenolic resin dispersed particle gel for in-depth profile control in low permeability reservoirs. J. Petrol. Sci. Eng. 161, 703–714. https://doi.org/10.1016/j.petrol.2017.11.070.